

Experimental determination of the $R(5d)$ - $T(3d)$ hybridization in rare-earth intermetallics

M. A. Laguna-Marco, J. Chaboy, and C. Piquer

Instituto de Ciencia de Materiales de Aragón, CSIC-Universidad de Zaragoza, 50009 Zaragoza, Spain

(Received 12 November 2007; published 27 March 2008)

We present an x-ray magnetic circular dichroism (XMCD) study performed at the $R L_2$ edge in RAI_2 and RT_2 ($T=Fe, Co$) intermetallic compounds. By analyzing the modification of the XMCD spectra as both the rare earth and the alloyed element (Al, Fe, or Co) are changed in the compound, an extra contribution, $XMCD_T$, has been identified and undoubtedly associated with the $R(5d)$ - $T(3d)$ hybridization in Fe and Co compounds. The sign and intensity of this contribution are found to be related to the magnetism of the T neighboring atoms as well as to the strength of the T - R interaction. These findings open the possibility of experimentally quantifying both the $R(4f)$ - $R(5d)$ and the $T(3d)$ - $R(5d)$ hybridizations, which govern the R - T interaction.

DOI: [10.1103/PhysRevB.77.125132](https://doi.org/10.1103/PhysRevB.77.125132)

PACS number(s): 78.70.Dm, 61.05.cj, 75.50.Bb

I. INTRODUCTION

Rare-earth (R) transition-metal (T) intermetallics have received great attention in the last decades owing to their technological significance as permanent magnets. However, the full understanding of the magnetic properties of these compounds is still missing. It needs the experimental determination of the magnetic coupling between $R(4f)$ and $T(3d)$ moments. In particular, the determination of the role played by the rare-earth $5d$ states, $R(5d)$, and their hybridization with the $3d$ states of the transition metal, $T(3d)$, is a fundamental question which has not been solved to date.

This goal has motivated a large quantity of work from both theoretical and experimental points of view since the 1970s. More recently, the development of the X-ray magnetic circular dichroism (XMCD) technique triggered a renewed interest in the field.^{1,2} In principle, the XMCD technique can provide the experimental magnetic characterization of $R(5d)$ states through the analysis of the $R L_{2,3}$ -edge XMCD spectra. Unfortunately, the XMCD expectations focused on disentangling of the magnetic contribution of the $5d$ and $4f$ states in lanthanides have not been fulfilled. The sign and magnitude of the XMCD signals at the $R L_{2,3}$ absorption edges are affected by the contribution of quadrupolar ($2p \rightarrow 4f$) transitions^{3,4} and by the spin dependence of the radial matrix elements of the dipolar ($2p \rightarrow 5d$) transitions.^{5,6} Consequently, the interpretation of the XMCD spectra at these edges is not straightforward and no direct correlation between the XMCD and the $5d$ magnetic moment has been established up to now.

The search of the whole understanding of the XMCD at the $L_{2,3}$ spectra of the rare earths led to the proposition of different theoretical models⁷⁻⁹ whose performance has been recently discussed by Giorgetti *et al.*² In the particular case of R -Fe intermetallics, recent theoretical works suggest the need of including the $R(5d)$ -Fe($3d$) hybridization to account for the $R L_{2,3}$ -XMCD, although this contribution is added *ad hoc* for different compounds.^{10,11} Notwithstanding the above results indicate that the $R(5d)$ magnetic moments cannot be determined from the $L_{2,3}$ -XMCD; its sensitivity to the interatomic hybridization may offer an experimental way to obtain new physical information about the $T(3d)$ - $R(5d)$ hybridization.

In this paper, we address this problem in connection with the binary RAI_2 , RCO_2 , and RFe_2 compounds, whose macroscopic properties are well known. Since the $R(5d)$ states are known to be hybridized with both $R(4f)$ and $T(3d)$ states, we have performed a systematic study of the L_2 -edge XMCD spectrum in different RAI_2 , RCO_2 , and RFe_2 compounds aimed to prove how these signals are sensitive to the effect of $R(4f)$ - $R(5d)$ and $T(3d)$ - $R(5d)$ hybridizations. Our results show the presence of an *extra* magnetic contribution, $XMCD_T$, associated with the transition metal even when the rare earth is probed. Moreover, a clear correlation has been established between $XMCD_T$ and both the magnetic state of the T element and the strength of the R - T interaction. These results suggest that XMCD can be used to get direct experimental information on the $T(3d)$ - $R(5d)$ hybridization and its role in the R - T interaction that determines the magnetic properties of these intermetallic compounds.

II. EXPERIMENT

Rare-earth L_2 -edge XMCD experiments were performed at the beamline BL39XU of the SPring-8 facility.¹² XMCD spectra were recorded in the transmission mode using the helicity-modulation technique.¹³ The spin-dependent absorption coefficient was obtained as the difference of the X-ray absorption spectroscopy (XAS) spectra for antiparallel and parallel orientations of the photon helicity and sample magnetization. In all the cases, the origin of the energy scale was chosen at the inflection point of the absorption edge and the XAS spectra were normalized to the averaged absorption coefficient at high energy. The macroscopic magnetic measurements, $M(T)$ and $M(H)$, were recorded by using a commercial superconducting quantum interference device magnetometer (Quantum Design MPMS-S5). For temperatures above ambient, $M(T)$ measurements were recorded by using a Faraday-type balance. The Curie temperature T_C was determined as the inflection point of the $M(T)$ curves. Details of sample preparation and characterization can be found elsewhere.^{1,14}

III. RESULTS AND DISCUSSION

The XMCD spectra measured at the $R L_2$ edge on the binary Laves phases RAI_2 , RFe_2 , and RCO_2 , at 5 K and under

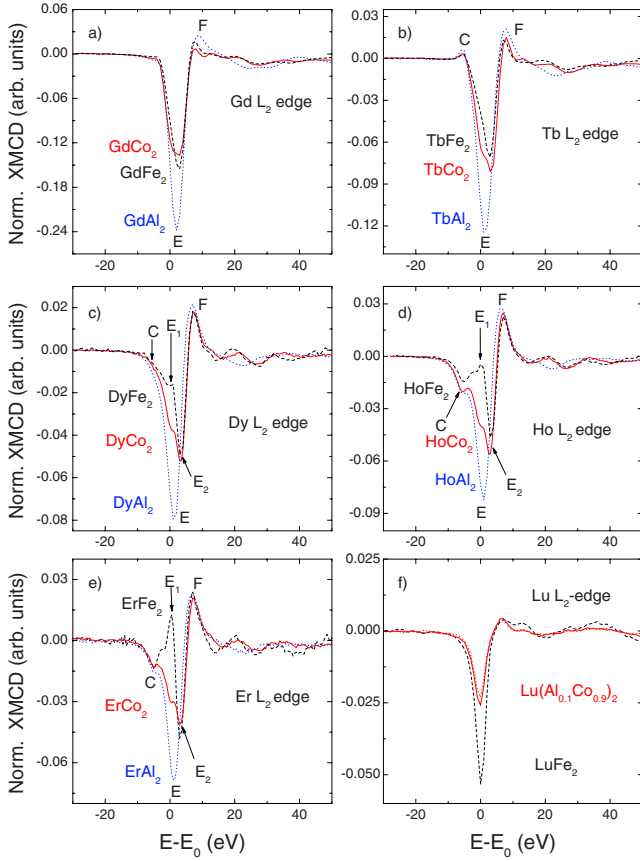


FIG. 1. (Color online) R L_2 -edge XMCD spectra recorded at $T=5$ K and $H=50$ kOe on RAl_2 (blue dotted line), RFe_2 (black dashed), and RCo_2 (red solid). XMCD spectra on $Lu(Al_{0.1}Co_{0.9})_2$ at $T=5$ K, $H=100$ kOe (red solid line) and $T=5$ K, $H=30$ kOe (red dotted line) are also included.

an applied magnetic field of 50 kOe, are displayed in Fig. 1. The spectral profile of RAl_2 consists of a main negative peak centered at $E-E_0 \sim 2$ eV above the edge (E) and a smaller positive peak at higher energy, $E-E_0 \sim 7$ eV (F). In addition to the main spectral features, $DyAl_2$, $HoAl_2$, and $ErAl_2$ present a negative shoulder at $E-E_0 \sim -5$ eV, while in the case of Tb, a small positive peak appears at this energy (C).

When the $3d$ metal is placed in the lattice, both the shape and the amplitude of the XMCD spectra are strongly modified with respect to those of the RAl_2 compounds. The modification of the amplitude does not occur equally through the whole energy range. Thus, feature F is slightly affected, while the amplitude of the main negative peak E is dramatically reduced. Moreover, the low energy part of peak E (E_1) undergoes a more abrupt decrease than higher energy part (E_2). As a result, the shape of this feature evolves from a single negative peak in RAl_2 to a more structured profile showing two components when the $3d$ metals are present. Furthermore, it can be seen in Fig. 1 that, despite the same kind of modification holds for both the Co and Fe Laves phases, the reduction at E_1 is clearly more obvious in the case of Fe compounds. This modification of the profile of

TABLE I. Magnetic parameters of the RAl_2 , RFe_2 , RCo_2 , and $Lu(Al_{0.1}Co_{0.9})_2$ compounds: M is the magnetization measured at $T=5$ K and $H=5$ kOe and T_C is the Curie temperature obtained as the inflection point of the experimental $M(T)$ curves. PM—paramagnetic compound.

Sample	M (μ_B /f.u.)	T_C (K)
YFe_2	2.87	541
YCo_2	...	PM
$GdFe_2$	3.91	793
$GdCo_2$	5.00	400
$GdAl_2$	7.00	164
$TbFe_2$	4.79	653
$TbCo_2$	6.32	235
$TbAl_2$	8.70	109
$DyFe_2$	6.45	628
$DyCo_2$	7.46	150
$DyAl_2$	9.45	58
$HoFe_2$	6.54	606
$HoCo_2$	7.98	78
$HoAl_2$	9.25	28
$ErFe_2$	5.57	582
$ErCo_2$	7.15	32
$ErAl_2$	7.90	13
$LuFe_2$	2.86	582
$LuCo_2$...	PM
$Lu(Al_{0.1}Co_{0.9})_2$	1.16	90

peak E is more clearly observed in the case of $DyFe_2$, $HoFe_2$, and $ErFe_2$ compounds. Indeed, $ErFe_2$ not only presents a reduction of E_1 but a positive peak at energy of ~ 0 eV.

The different R L_2 -edge XMCD profile observed for RAl_2 , RFe_2 , and RCo_2 cannot be explained in terms of the current knowledge of the XMCD signals at the R $L_{2,3}$ absorption edges. The commonly accepted description states that the shape and the amplitude are governed by the $4f$ magnetism through the intra-atomic $R(4f)$ - $R(5d)$ hybridization.⁵ In the RT_2 series of compounds, the $4f$ magnetic moment is commonly assumed to be close to the free-ion values in all the studied compounds, in agreement with magnetization data (see Table I). Consequently, no significant variation of the intra-atomic $R(4f)$ - $R(5d)$ polarization effect is expected and the experimental behavior of the XMCD cannot be explained in terms of a different $4f$ magnetism through the three series. On the contrary, the fact that the magnetic properties of the R counterpart (Al, Fe, and Co) are clearly different suggests that the origin of such a behavior stems from an unexpected magnetic contribution arising from the T sublattice even if the R is probed. Indeed, these results, showing evidence of the influence of the magnetic $3d$ atoms at the R L_2 -XMCD,

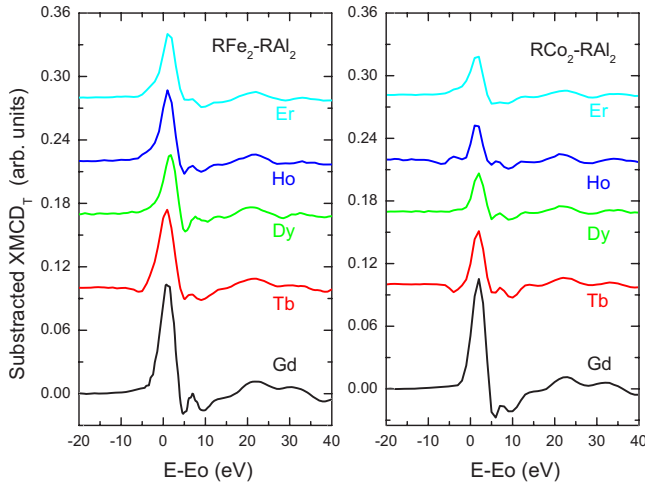


FIG. 2. (Color online) XMCD_T signal obtained after subtraction, $\text{XMCD}_{RT_2} - \text{XMCD}_{RAl_2}$.

are in agreement with previous findings in the $R(\text{Al}_{1-x}\text{Fe}_x)_2$ and $R(\text{Al}_{1-x}\text{Co}_x)_2$ series.^{1,15} In these cases, it was found that as Al is replaced by magnetic atoms (Fe or Co), a new contribution emerges whose intensity, gradually evolving as a function of the Al(*T*) content, is related to the number of 3*d* atoms surrounding the absorbing rare-earth atom, as well as to the value of the magnetic moment of the specific transition metal in the compound.^{1,15}

In order to isolate the *T* contribution to the $R L_2$ -XMCD, we have subtracted from each recorded dichroic spectrum that of RAl_2 with the same *R*. That is, $\text{XMCD}_T = \text{XMCD}_{RT_2} - \text{XMCD}_{RAl_2}$. In other words, we have considered that the XMCD spectra measured at the $R L_2$ edge on *R-T* systems are made up of two magnetic contributions: one of *R* origin and the other of *T* origin. According to the previously discussed models, the rare-earth contribution to the $R L_2$ -XMCD spectrum, XMCD_R , is determined by the 4*f* states through both the quadrupolar transition and the spin dependence of the radial matrix elements of the dipolar transition arising from the intra-atomic $R(4f)$ - $R(5d)$ hybridization. Due to its atomiclike nature, the 4*f* magnetic moment of the RT_2 compounds remains near unchanged for a fixed rare earth. Therefore, it is expected that the 4*f* contribution, XMCD_R , does not change by varying *T*. By assuming that this contribution corresponds to that of the RAl_2 compounds, the subtraction procedure above allows one to disentangle the magnetic contribution of the transition metal, XMCD_T , to the rare-earth L_2 -XMCD spectrum. The result of applying this subtraction procedure is shown in Fig. 2. The subtracted signal is mainly made of a very intense positive peak, at $E-E_0 \sim 0$ eV, followed by a small structured negative peak at higher energies. As it can be seen, the profile is basically the same no matter the rare earth nor the transition metal.

In order to go further into the origin of the emerging component, we have born in mind the mechanism of the magnetic coupling in these materials, where the $R(5d)$ - $T(3d)$ hybridization plays a critical role.^{16–18} The influence of the $T(3d)$ states into the $R(5d)$ magnetism is demonstrated by the existence of $R L_{2,3}$ dichroism in *R-T* compounds, where *R* is non magnetic as Lu.¹⁹ Taking into account that the Lu

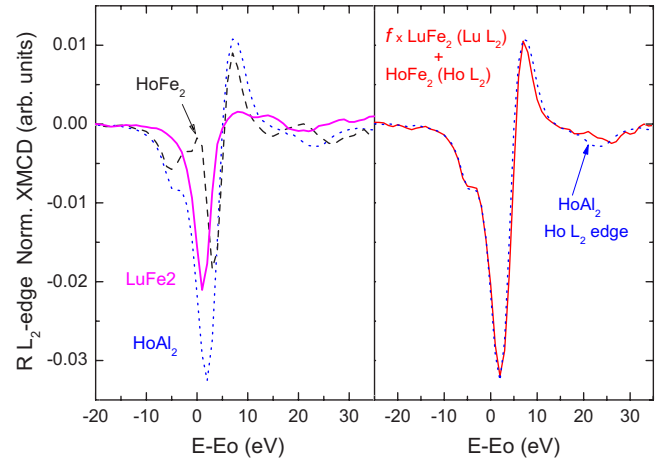


FIG. 3. (Color online) Comparison of the $R L_2$ -edge XMCD spectra recorded on HoAl_2 (blue dotted line), HoFe_2 (black dashed), LuFe_2 (magenta), and the XMCD spectrum obtained as the addition of HoFe_2 and LuFe_2 (red). A factor ($f=1.2$ in this case) is necessary to meet both profiles.

magnetic signal cannot arise from the $R(4f)$ - $R(5d)$ hybridization, as Lu has its 4*f* band complete filled, the appearance of a nonzero XMCD signal at the Lu L_2 edge has to be explained in terms of the polarization of the $R(5d)$ states induced by the $T(3d)$ moments. Moreover, if this hypothesis is correct, the Lu L_2 XMCD signal will be proportional to μ_T . Therefore, we have recorded the $R L_2$ -edge XMCD spectra in the Laves phases containing a nonmagnetic rare earth: LuFe_2 and $\text{Lu}(\text{Al}_{0.1}\text{Co}_{0.9})_2$.²⁰ As shown in Fig. 1(f), the intensity of the LuFe_2 signal is about twice that of the Co compound, in agreement with the different values of μ_{Fe} ($2.86\mu_B$ for LuFe_2) and μ_{Co} [$1.16\mu_B$ for $\text{Lu}(\text{Al}_{0.1}\text{Co}_{0.9})_2$] obtained from macroscopic magnetic data at $H=50$ kOe.

The comparison of the subtracted signals to the Lu L_2 -edge spectra of LuFe_2 and $\text{Lu}(\text{Co}_{0.9}\text{Al}_{0.1})_2$ compounds reports some other important results: (i) the Lu XMCD spectrum appears at the same $E-E_0$ energy where the “*T* contribution” is located in the RT_2 cases, (ii) the profile of the subtracted signals closely resembles the Lu signals, and (iii) in the case of Lu samples, the L_2 XMCD spectrum is negative, while the subtracted signal is positive. This is in agreement with the opposite direction of $\mu_{\text{Fe}(\text{Co})}$ relative to the total magnetization of the sample for Lu and heavy magnetic rare-earth samples.

There is no reason for the disappearance of the influence of the 3*d* moments when the *R* carries a 4*f* magnetic moment. Consequently, the magnetism of the 5*d* states results from the interplay of both $R(4f)$ - $R(5d)$ and $T(3d)$ - $R(5d)$ polarizations, giving rise to two different contributions to the XMCD spectrum at the $R L_{2,3}$ edges. To illustrate to what extent this schematic two sublattice picture is suitable for describing the XMCD spectra at the L_2 edge in the case of *R-T* intermetallics, we have “rebuilt” the spectrum of RAl_2 by the addition of RT_2 and LuT_2 signals. In Fig. 3, the result of such a procedure has been plotted for Ho compounds. As it can be seen, the experimental HoAl_2 spectra match with the profile obtained by applying a two $\text{HoFe}_2 + f \text{LuFe}_2$ sublattice model. A similar result is obtained for all the RT_2

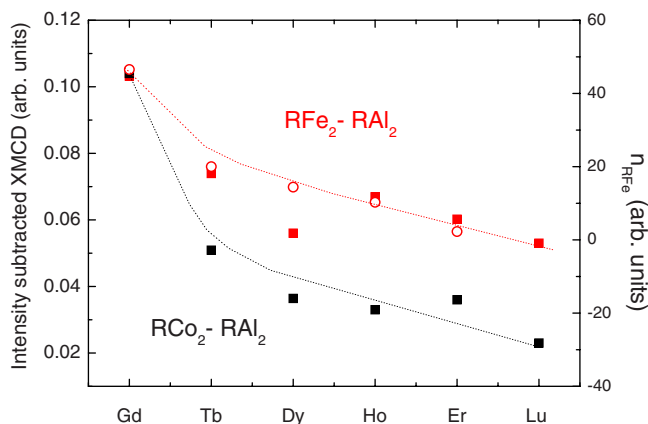


FIG. 4. (Color online) Comparison of the intensity of the XMCD_T signal (Fe series: ■; Co series: ■). In a different scale, the modification of the n_{RFe} coefficient calculated from $M(T)$ curves is also included (○). Dotted lines are guides for the eyes.

compounds. f is a factor necessary to meet the profiles. It ranges from 1.1 ErFe_2 in to 1.7 in GdFe_2 .

Moreover, the comparison of the intensity of XMCD_T for the different measured compounds (Fig. 4) shows that the size of the Fe contribution is 1.4–2 times that obtained for the Co Laves phases. As the Fe magnetic moment, $\sim 1.6\mu_B$, is about twice larger than the Co magnetic moment, $\sim 0.9\mu_B$, in the RT_2 Laves phases, this result confirms that the emerging peak is related with a magnetic contribution stemming from the $3d$ metal.

The XMCD_T signal also presents, as a general trend, a reduction as the atomic number of the rare earth increases. Given that μ_{Fe} can be regarded as constant through the binary $R\text{Fe}_2$ series, the evolution of the intensity of the XMCD_{Fe} signal presented in Fig. 4 can hardly be explained in terms of a modification of μ_{Fe} . Even if we assume that μ_{Fe} varies from LuFe_2 ($1.45\mu_B$) to GdFe_2 ($\sim 1.60\mu_B$),²¹ this increase is too small to account for the clear difference observed in the intensity of the subtracted signal. Therefore, different arguments have to be investigated to explain the intensity modification induced by the substitution of the rare earth. Taking into account the proposed origin of XMCD_T , its modification must be related to changes in the $T(3d)$ - $R(5d)$ hybridization. Band-structure calculations show that the decreasing lattice constant with the atomic number Z leads to an enhancement of the $T(3d)$ - $R(5d)$ hybridization.²² Therefore, this volume effect alone would not explain the decrease of the T contribution. A further point to be considered is the fact that the strength of the $T(3d)$ - $R(5d)$ hybridization will also be affected by the polarization of the $R(5d)$ states due to the $R(4f)$ shell. At this point, it is interesting to note that the R - T interaction is considered to be strongly affected by the intratomic $R(4f)$ - $R(5d)$ exchange. In view of the indirect nature of the R - T interaction, Belorizki *et al.*²³ explained the decrease of the molecular field coefficient n_{RT} across the lanthanide series in terms of the reduction of the $R(4f)$ - $R(5d)$ hybridization. The reduction of the atomic radius of the R ion with increasing Z is much weaker (about ten times) than the decrease of the $4f$ shell, leading to a smaller overlap of the $4f$ and $5d$ shells with increasing Z . In

addition, they conclude that the variation of the $T(3d)$ - $R(5d)$ hybridization through the series is negligible in a first approximation. Following this argument, we have included the modification of n_{RFe} into the comparison in Fig. 4. The n_{RFe} coefficients were calculated from the experimental T_C values following a standard procedure for intermetallic compounds.²⁴ Both the intensity of the dichroic signal and n_{RT} show the same trend which suggests the common origin of XMCD_T and n_{RT} . This relationship between XMCD_T and n_{RT} has not been previously reported. It also explains the need of including a factor f in Fig. 3.

Regarding the Co Laves series, we cannot apply the same procedure and make a comparison between the intensity of the XMCD signal and n_{RT} obtained from T_C values due to the particular behavior of Co in this series.²⁰ Indeed, the magnetism of the Co sublattice is strongly dependent on the specific R element in the alloy. Thus, LuCo_2 is paramagnetic, whereas $R\text{Co}_2$ compounds with a heavy rare earth are ferromagnets showing a Co moment of $\sim 0.9\mu_B$. On the other hand, $\text{Lu}(\text{Al}_{0.1}\text{Co}_{0.9})_2$ shows a higher T_C than HoCo_2 and ErCo_2 . Nevertheless, values of the exchange interaction presented by Duc and Brommer²⁵ indicate a diminution with increasing atomic number across the $R\text{Co}_2$ series, which is in agreement with our results presented in Fig. 4.

A final comment is deserved to the different contribution of the transition metal to the XMCD recorded at the L_2 and L_3 absorption edges of the rare earths. In the case of the L_3 edge spectra, the same trend has not been observed. The origin of these differences has been discussed in Ref. 26.

IV. SUMMARY AND CONCLUSIONS

Summarizing, we have performed an XMCD study at the $R L_2$ edge in the $R\text{Al}_2$, $R\text{Fe}_2$, and $R\text{Co}_2$ series. In the light of our results, the XMCD signal measured at the $R L_2$ edge in compounds with two magnetic sublattices, R and T , can be regarded as consisting of the addition of two different contributions. These contributions emerge as a consequence of the polarization of the $5d$ states by both the $R(4f)$ ones, through an intratomic exchange, and the $3d$ states of the transition metal, through the $T(3d)$ - $R(5d)$ hybridization. The transition-metal contribution has been isolated and shown to be related with both the number of T neighbors around the absorbing R (Ref. 1) and the magnetic moment (both magnitude and sign) of the transition metal in the compound μ_T . Moreover, there is a good agreement between the modification of both XMCD_T and the molecular field coefficient n_{RT} through the RT_2 series. This result indicates that this XMCD analysis well may be further used to get an experimental determination of the $T(3d)$ - $R(5d)$ hybridization. Such an information is not visible in macroscopic measurements and, as a result, it has not been obtained to date. This information is of fundamental importance not only to get a correct interpretation of the $R L_{2,3}$ XMCD signals but also to provide a full understanding of the magnetism of R - T intermetallics.

ACKNOWLEDGMENTS

This work was partially supported by Spanish CICYT-MAT2005-06806-C04-04 grant. The synchrotron radiation experiments were performed at SPring-8 (Proposals No.

2003B0064-NSc-np and No. 2005B0419). We are indebted to H. Maruyama and N. Kawamura for their help during the experimental work at Spring-8. M.A. Laguna-Marco acknowledges MEC for Ph.D. grant.

-
- ¹M. A. Laguna-Marco, J. Chaboy, C. Piquer, H. Maruyama, N. Ishimatsu, N. Kawamura, M. Takagaki, and M. Suzuki, *Phys. Rev. B* **72**, 052412 (2005), and references therein.
- ²C. Giorgetti, E. Dartyge, F. Baudelet, and R.-M. Galéra, *Phys. Rev. B* **70**, 035105 (2004), and references therein.
- ³J. C. Lang, S. W. Kycia, X. D. Wang, B. N. Harmon, A. I. Goldman, D. J. Branagan, R. W. McCallum, and K. D. Finkelstein, *Phys. Rev. B* **46**, 5298 (1992); J. C. Lang, G. Srajer, C. Detlefs, A. I. Goldman, H. König, X. Wang, B. N. Harmon, and R. W. McCallum, *Phys. Rev. Lett.* **74**, 4935 (1995).
- ⁴J. Chaboy, F. Bartolomé, L. M. García, and G. Cibir, *Phys. Rev. B* **57**, R5598 (1998).
- ⁵X. Wang, T. C. Leung, B. N. Harmon and P. Carra, *Phys. Rev. B* **47**, 9087 (1993).
- ⁶B. N. Harmon and A. J. Freeman, *Phys. Rev. B* **10**, 1979 (1974).
- ⁷T. Jo and S. Imada, *J. Phys. Soc. Jpn.* **62**, 3721 (1993).
- ⁸H. Matsuyama, I. Harada, and A. Kotani, *J. Phys. Soc. Jpn.* **66**, 337 (1997).
- ⁹M. van Veenendaal, J. B. Goedkoop, and B. T. Thole, *Phys. Rev. Lett.* **78**, 1162 (1997).
- ¹⁰K. Fukui, H. Ogasawara, A. Kotani, I. Harada, H. Maruyama, N. Kawamura, K. Kobayashi, J. Chaboy, and A. Marcelli, *Phys. Rev. B* **64**, 104405 (2001).
- ¹¹K. Asakura, J. Nakahara, I. Harada, H. Ogasawara, K. Fukui, and A. Kotani, *J. Phys. Soc. Jpn.* **71**, 2771 (2002).
- ¹²H. Maruyama, M. Suzuki, N. Kawamura *et al.*, *J. Synchrotron Radiat.* **6**, 1133 (1999).
- ¹³M. Suzuki, N. Kawamura, M. Mizumaki, A. Urata, H. Maruyama, S. Goto, and T. Ishikawa, *Jpn. J. Appl. Phys., Part 2* **37**, L1488 (1998).
- ¹⁴M. A. Laguna-Marco, Ph.D. thesis, Prensas Universitarias de Zaragoza, 2007.
- ¹⁵M. A. Laguna-Marco, J. Chaboy, C. Piquer, H. Maruyama, N. Ishimatsu, and N. Kawamura, *X-ray Absorption Fine Structure-XAFS13*, edited by B. Hedman and P. Painetta, AIP. Conf. Proc. No. 882 (AIP, New York, 2007) p. 484.
- ¹⁶H. Yamada and M. Shimizu, *J. Phys. F: Met. Phys.* **15**, L175 (1985).
- ¹⁷M. S. S. Brooks, O. Eriksson, and B. Johansson, *J. Phys.: Condens. Matter* **1**, 5861 (1989).
- ¹⁸M. S. S. Brooks, L. Nordström and B. Johansson, *J. Phys.: Condens. Matter* **3**, 2357 (1991).
- ¹⁹F. Baudelet, C. Brouder, E. Dartyge, A. Fontaine, J. P. Kappler, and G. Krill, *Europhys. Lett.* **13**, 751 (1990).
- ²⁰The XMCD signal of Lu(Al_{0.1}Co_{0.9})₂ has been measured instead of that of LuCo₂ due to the Pauli paramagnetism of LuCo₂. A small substitution of Co by Al renders these compound itinerant ferromagnets. See, for example, I. S. Dubenko, R. Z. Levitin, A. S. Markosyan, and H. Yamada, *J. Magn. Magn. Mater.* **136**, 93 (1994), and references therein.
- ²¹E. Burzo, *Solid State Commun.* **20**, 569 (1976).
- ²²J. P. Lui, F. R. de Boer, P. F. de Chatel, R. Coehoorn, and K. H. J. Buschow, *J. Magn. Magn. Mater.* **132**, 159 (1994).
- ²³E. Belorizky, M. A. Fremy, J. P. Gavigan, D. Givord, and H. S. Li, *J. Appl. Phys.* **61**, 3971 (1987).
- ²⁴See, for example, K. H. J. Buschow, in *Supermagnets: Hard Magnetic Materials*, edited by G. J. Long and F. Grandjean (Kluwer, Dordrecht, 1991).
- ²⁵N. H. Duc and P. E. Brommer, in *Handbook of Magnetic Materials*, edited by K. H. J. Buschow (Elsevier Science, New York, 1999), Vol. 12.
- ²⁶J. Chaboy, M. A. Laguna-Marco, C. Piquer, H. Maruyama, and N. Kawamura, *J. Phys.: Condens. Matter* **19**, 436225 (2007).